CONVERGENCE ANALYSIS OF THE VARIATIONAL OPERATOR SPLITTING SCHEME FOR A REACTION-DIFFUSION SYSTEM WITH DETAILED BALANCE*

CHUN LIU†, CHENG WANG‡, YIWEI WANG§, AND STEVEN M. WISE¶

Abstract. We present a detailed convergence analysis for an operator splitting scheme proposed in [C. Liu, C. Wang, and Y. Wang, *J. Comput. Phys.*, 436 (2021), 110253] for a reaction-diffusion system with detailed balance. The numerical scheme has been constructed based on a recently developed energetic variational formulation, in which the reaction part is reformulated in terms of the reaction trajectory, and both the reaction and diffusion parts dissipate the same free energy. The scheme is energy stable and positivity-preserving. In this paper, the detailed convergence analysis and error estimate are performed for the operator splitting scheme. The nonlinearity in the reaction trajectory equation, as well as the implicit treatment of nonlinear and singular logarithmic terms, impose challenges in numerical analysis. To overcome these difficulties, we make use of the convex nature of the logarithmic nonlinear terms. In addition, a combination of rough error estimate and refined error estimate leads to a desired bound of the numerical error in the reaction stage, in the discrete maximum norm. Furthermore, a discrete maximum principle yields the evolution bound of the numerical error function at the diffusion stage. As a direct consequence, a combination of the numerical error analysis at different stages and the consistency estimate for the operator splitting procedure results in the convergence estimate of the numerical scheme for the full reaction-diffusion system. The convergence analysis technique could be extended to a more general class of dissipative reaction mechanisms. As an example, we also consider a near-equilibrium reaction kinetics, which was derived by the linear response assumption on the reaction trajectory. Although the reaction rate is more complicated in terms of concentration variables, we show that the numerical approach and the convergence analysis also work in this case.

1. Introduction. Reaction-diffusion-type equations have wide applications in modeling many physical and biological systems, such as pattern formation [26, 32, 46], tumor growth [28, 39, 47], molecular motors [9, 30, 53], and active materials [48, 55]. For simplicity of presentation, we consider a reaction-diffusion system with three

†Department of Applied Mathematics, Illinois Institute of Technology, Chicago, IL 60616 USA (cliu124@iit.edu).
‡Department of Mathematics, University of Massachusetts Dartmouth, North Dartmouth, MA 02747-2300 USA (cwang1@umassd.edu).
§Corresponding author. Department of Applied Mathematics, Illinois Institute of Technology, Chicago, IL 60616 USA (ywang487@iit.edu).
¶Department of Mathematics, University of Tennessee, Knoxville, TN 37996 USA (swise1@utk.edu).

reactive components:

$$(1.1) \qquad \begin{cases} \partial_t a = \nabla \cdot (D_a(\mathbf{x})\nabla a) - ab + c, \\ \partial_t b = \nabla \cdot (D_b(\mathbf{x})\nabla b) - ab + c, \\ \partial_t c = \nabla \cdot (D_c(\mathbf{x})\nabla c) + ab - c, \end{cases}$$

subject to a periodic boundary condition and a positive initial condition

$$(a(\mathbf{x},0), b(\mathbf{x},0), c(\mathbf{x},0)) = (a_0(\mathbf{x}), b_0(\mathbf{x}), c_0(\mathbf{x})) \in \mathbb{R}^{3,+}.$$

Here a, b, and c are concentrations of species A, B, and C, and $D_\alpha(\mathbf{x}) > 0$ $(\alpha = a, b, c)$ are diffusion coefficients. System (1.1) is associated to a chemical reaction $A + B \underset{k^-}{\overset{k^+}{\rightleftharpoons}} C$, with $k^+ = k^- = 1$.

The original reaction-diffusion system (1.1) is not a gradient flow, at least not in a direct form. As a result, standard numerical methodologies for gradient flows are not directly applicable to this system. Fortunately, some recent works [35, 37, 54] have discovered that the reaction and diffusion parts correspond to two different, but complimentary, gradient flow structures. Although these two gradient flow structures are very different, they share exactly the same free energy.

Indeed, letting $a^\infty > 0$, $b^\infty > 0$, and $c^\infty > 0$ satisfy

$$(1.2) \qquad k^+ a^\infty b^\infty = k^- c^\infty,$$

with $k^+ = k^- = 1$ in the present case, we can define the free energy $\mathcal{F}(a,b,c)$ as
(1.3)
$$\mathcal{F}(a,b,c) := \int_\Omega \left(a\left(\ln\left(\frac{a}{a^\infty} \right) - 1 \right) + b\left(\ln\left(\frac{b}{b^\infty} \right) - 1 \right) + c\left(\ln\left(\frac{c}{c^\infty} \right) - 1 \right) \right) d\mathbf{x}.$$

The corresponding chemical potentials, μ_A, μ_B, and μ_C, for species A, B, and C associated to the free energy $\mathcal{F}(a,b,c)$, can be calculated as

$$(1.4) \qquad \mu_A := \frac{\delta \mathcal{F}}{\delta a} = \ln \frac{a}{a^\infty}, \quad \mu_B := \frac{\delta \mathcal{F}}{\delta b} = \ln \frac{b}{b^\infty}, \quad \mu_C := \frac{\delta \mathcal{F}}{\delta c} = \ln \frac{c}{c^\infty}.$$

For the reaction-only part

$$(1.5) \qquad \partial_t a = -ab + c, \quad \partial_t b = -ab + c, \quad \partial_t c = ab - c,$$

one can introduce a new variable,

$$R(\mathbf{x},t) = \int_0^t (ab - c)\, ds,$$

known as the reaction trajectory [54]. The reaction trajectory $R(\mathbf{x},t)$, which was originally introduced by De Donder [10] as a state variable for a chemical reaction system, accounts for the number of forward reaction which has happened by time t. In turn, one gets $a = a_0 - R$, $b = b_0 - R$, $c = c_0 + R$, and the following equation of R could be derived [54]:

$$\ln\left(1 + \frac{\partial_t R}{c} \right) = \ln\left(1 + \frac{ab - c}{c} \right) = \ln\left(\frac{ab}{c} \right) = \ln a + \ln b - \ln c$$
$$(1.6) \qquad\qquad = \ln(a_0 - R) + \ln(b_0 - R) - \ln(c_0 + R).$$

The free energy can be written in terms of R, specifically, $\mathcal{F}(a, b, c) = \tilde{\mathcal{F}}(R)$, and it is easy to see that

$$(1.7) \qquad \ln\left(1 + \frac{\partial_t R}{c}\right) = \ln(a_0 - R) + \ln(b_0 - R) - \ln(c_0 + R) = -\frac{\delta \tilde{\mathcal{F}}}{\delta R}.$$

Therefore, the following energy dissipation law is available:

$$\frac{\mathrm{d}}{\mathrm{d}t}\tilde{\mathcal{F}}(R) = \left(\partial_t R, \frac{\delta \tilde{\mathcal{F}}}{\delta R}\right) = -\left(c\frac{\partial_t R}{c}, \ln\left(1 + \frac{\partial_t R}{c}\right)\right) \le 0,$$

provided that $\frac{\partial_t R}{c} > -1$. In other words, the reaction part becomes a generalized gradient flow in terms of R, which is decidedly different from the standard L^2 or H^{-1} gradient flow structures. The monotonicity of $\ln(1 + \frac{\partial_t R}{c})$ (in terms of $\partial_t R$) for $c > 0$ plays an important role in the dissipation mechanism.

In the meantime, it is observed that the diffusion-only part,

$$(1.8) \qquad \partial_t a = \nabla \cdot (D_a(\mathbf{x})\nabla a), \quad \partial_t b = \nabla \cdot (D_b(\mathbf{x})\nabla b), \quad \partial_t c = \nabla \cdot (D_c(\mathbf{x})\nabla c),$$

could be rewritten as the following H^{-1} gradient flow, with nonconstant mobility:

$$(1.9) \quad \partial_t a = \nabla \cdot (D_a(\mathbf{x})a\nabla \mu_A), \quad \partial_t b = \nabla \cdot (D_b(\mathbf{x})b\nabla \mu_B), \quad \partial_t c = \nabla \cdot (D_c(\mathbf{x})c\nabla \mu_C).$$

This gradient flow structure is similar to that of the Poisson–Nernst–Planck (PNP) system [38, 49].

As a consequence, the overall system satisfies the energy-dissipation law [54]:

$$
\begin{aligned}
(1.10) \qquad \frac{\mathrm{d}}{\mathrm{d}t}\mathcal{F}(a, b, c) = &-\int_\Omega D_a(\mathbf{x})a|\nabla \mu_A|^2 + D_b(\mathbf{x})b|\nabla \mu_B|^2 + D_c(\mathbf{x})c|\nabla \mu_C|^2 \\
&+ \partial_t R \ln\left(1 + \frac{\partial_t R}{c}\right)\mathrm{d}\mathbf{x} \le 0.
\end{aligned}
$$

Remark 1.1. There have been many existing works aiming to establish a variational structure of reaction-diffusion systems [2, 14, 15, 25, 27, 41, 42, 35, 50, 56, 54]. Condition (1.2) is known as the *detailed balance* condition, which guarantees the existence of the free energy [2, 15]. We call (1.10) the energetic variational formulation for the reaction-diffusion system, which can be used to model the coupling between a general reversible reaction network and another mechanical process, such as general diffusions. We refer interested readers to [37, 54] for the energetic variational formulation for more general cases.

Although the reaction and diffusion parts in (1.1) correspond to very different gradient flow structures, their free energy functionals are exactly the same. If one applies a standard numerical discretization to the original reaction-diffusion system (1.1), the variational structure may be lost. In turn, either the theoretical property or the logarithmic energy stability could not be justified. This fact motivates the development of the operator splitting scheme [37], in which the reaction stage is solved in terms of the reaction trajectory R and both stages dissipate the same discrete energy. The unique solvability, positivity-preserving property and energy stability have been theoretically established for the proposed operator splitting scheme. However, its convergence analysis and error estimate remain open, in which the primary difficulty comes from the nonlinear and singular nature of the logarithmic terms. The implicit treatment of

these nonlinear and singular logarithmic terms are crucial to enforcing the positivity of the numerical solution, as well as the energy stability analysis, while it has posed a great challenge in the theoretical justification of the convergence analysis. Also see the related works [8, 16, 17, 18, 57] for the Cahn–Hilliard equation with Flory–Huggins energy potential, as well as [38, 49] for the PNP system, [19] for the porous medium equation, [60] for a liquid film droplet model, etc.

In this paper we provide a detailed convergence analysis and error estimate for the operator splitting scheme, proposed in [37] and applied to the reaction-diffusion system (1.1). A careful consistency estimate for the splitting process, as well as the temporal discretization at each stage, gives an $O(\Delta t)$ truncation error. In addition, the centered difference spatial discretization at the diffusion stage implies an $O(h^2)$ truncation error. To overcome the subtle difficulty associated with the singularity, we make use of the convex nature of the logarithmic nonlinear terms, which are implicitly treated in the reaction stage. In addition, a combination of rough error estimate and refined error estimate is performed in the reaction stage, which in turn leads to a desired bound of the numerical error in the discrete maximum norm. Moreover, a careful application of discrete maximum principle yields the evolution bound of the numerical error function at the diffusion stage. Therefore, a combination of the numerical error analysis at different stages results in the convergence estimate of the numerical scheme for the full reaction-diffusion system in the discrete maximum norm.

In addition, this convergence analysis technique could be extended to a more general class of reaction dissipation mechanism. The reaction rates in (1.1) stand for a special example of the law of mass action, i.e., the reaction rate is directly proportional to the product of the concentrations of the reactants. This law usually gives a simple form of the reaction rate in terms of concentration variables, while the dissipation in terms of R and R_t becomes more complicated. Alternatively, the linear response theory has been proposed and applied, which in turn leads to a more complicated reaction rate formula (in the singular logarithmic form) and simpler reaction dissipation (the standard L^2 gradient flow); see the more detailed derivations in [54]. The numerical schemes proposed in [37] focused on the reaction rate given by the law of mass action, while the reaction-diffusion system with the reaction dissipation given by the linear response theory was not covered in this reference. Meanwhile, the idea of operator splitting, the rough/refined error estimates in the reaction stage, as well as the maximum norm error estimate for the overall numerical scheme could be very effectively extended. In general, as long as the free energy is a singular and convex energy potential in terms of the reaction trajectory R, and the left-hand side of its evolutionary equation could be represented as a monotone function of R_t, these numerical analysis techniques will be applicable.

The rest of this paper is organized as follows. The positive-preserving and energy stable operator splitting scheme for the reaction-diffusion system (1.1) is reviewed in section 2. The optimal rate convergence analysis and error estimate are presented in section 3. The corresponding analysis for more generalized reaction dissipation mechanism, such as the one given by the linear response theory, is provided in section 4. A numerical result is given in section 5, which validates the theoretical analysis. Finally, some concluding remarks are made in section 6.

2. Review of the operator splitting numerical scheme. In this section, we give a brief review to the operator splitting method proposed in [37], which is based on the energetic variational formation (1.10) of (1.1). Letting $\mathbf{u}(\mathbf{x}, t) =$

$(a(\mathbf{x}, t), b(\mathbf{x}, t), c(\mathbf{x}, t))^{\mathrm{T}}$, the reaction-diffusion system (1.1) can be represented as

$$\text{(2.1)} \qquad \partial_t \mathbf{u}(\boldsymbol{x}, t) = \mathcal{A}\mathbf{u} + \mathcal{B}\mathbf{u},$$

where $\mathcal{A}$ and $\mathcal{B}$ are the reaction operator and the diffusion operator, respectively. As mentioned earlier, the key point of designing an energy-stable, positivity-preserving numerical scheme for the reaction part is to discretize the reaction trajectory equation (1.7) directly. We present the numerical algorithm on the computational domain $\Omega = (0, 1)^3$ with periodic boundary conditions and use a finite difference method as a spatial discretization. The spatial mesh size is set as $\Delta x = \Delta y = \Delta z = h = \frac{1}{N}$, where N is the spatial mesh resolution throughout this paper. In particular, $f_{i,j,k}$ stands for the numerical value of f at the cell centered mesh points $((i+\frac{1}{2})h, (j+\frac{1}{2})h, (k+\frac{1}{2})h)$, so that the discrete summation could be easily defined over Ω. The discrete gradient, divergence, and Laplacian operators, given by ∇_h, $\nabla_h\cdot$, and Δ_h, are defined based on the standard centered difference approximation. The discrete L^2 inner product between two grid functions f and g, as well as the discrete L^2 norm, are defined as

$$\text{(2.2)} \qquad \langle f, g \rangle := h^3 \sum_{i,j,k=1}^{N} f_{i,j,k} g_{i,j,k}, \quad \|f\|_2 := (\langle f, f \rangle)^{\frac{1}{2}}.$$

As an application, the discrete energy of a numerical solution (a, b, c) is introduced as

$$\text{(2.3)} \quad \mathcal{F}_h(a, b, c) := \left\langle a\left(\ln\left(\frac{a}{a^\infty}\right) - 1 \right) + b\left(\ln\left(\frac{b}{b^\infty}\right) - 1 \right) + c\left(\ln\left(\frac{c}{c^\infty}\right) - 1 \right), \mathbf{1} \right\rangle.$$

In addition to the discrete $\| \cdot \|_2$ norm, the discrete maximum norm is defined as follows:

$$\text{(2.4)} \qquad \|f\|_\infty := \max_{1 \le i,j,k \le N} |f_{i,j,k}|.$$

Based on the energy-dissipation law (1.10), the operator splitting scheme for (1.1) can be formulated as follows: Given a^n, b^n, c^n, with $a^n, b^n, c^n > 0$ at each mesh point, we update a^{n+1}, b^{n+1}, c^{n+1} via the following two stages.

Stage 1. First, we set $R^n \equiv 0$ and solve

$$\text{(2.5)}$$
$$\ln\left(\frac{R^{n+1} - R^n}{c^n \Delta t} + 1 \right) = \ln\left(\frac{a^n - R^{n+1}}{a^\infty} \right) + \ln\left(\frac{b^n - R^{n+1}}{b^\infty} \right) - \ln\left(\frac{c^n + R^{n+1}}{c^\infty} \right)$$

at each mesh point. By a careful analysis based on the convexity of the logarithmic function, one can show that there exists a unique solution R^{n+1} such that $a^n - R^{n+1} > 0$, $b^n - R^{n+1} > 0$, $c^n + R^{n+1} > 0$, and $R^{n+1} - R^n + c^n \Delta t > 0$. In turn, we denote

$$\text{(2.6)} \qquad a^{n+1,*} := a^n - R^{n+1}, \;\; b^{n+1,*} := b^n - R^{n+1}, \;\; c^{n+1,*} := c^n + R^{n+1}.$$

Furthermore, the following energy dissipation property has been established [37]:

$$\text{(2.7)} \qquad \mathcal{F}_h(a^{n+1,*}, b^{n+1,*}, c^{n+1,*}) \le \mathcal{F}_h(a^n, b^n, c^n).$$

Stage 2. The intermediate variables $a^{n+1,*}$, $b^{n+1,*}$, $c^{n+1,*}$ have been proved to be positive at each mesh point. Next, we update a^{n+1}, b^{n+1}, and c^{n+1} by the standard

implicit Euler scheme

$$(2.8) \quad \begin{cases} \dfrac{a^{n+1} - a^{n+1,*}}{\Delta t} = \nabla_h \cdot (D_a \nabla_h a^{n+1}), \\[2mm] \dfrac{b^{n+1} - b^{n+1,*}}{\Delta t} = \nabla_h \cdot (D_b \nabla_h b^{n+1}), \\[2mm] \dfrac{c^{n+1} - c^{n+1,*}}{\Delta t} = \nabla_h \cdot (D_c \nabla_h c^{n+1}), \end{cases}$$

where ∇_h and $\nabla_h \cdot$ are discrete gradient and divergence operators. The positivity and energy stability of the implicit Eulerian scheme has been proved in [37], i.e.,

$$(2.9) \qquad a^{n+1},\, b^{n+1},\, c^{n+1} > 0 \quad \text{(pointwise)},$$

$$(2.10) \qquad \mathcal{F}_h(a^{n+1}, b^{n+1}, c^{n+1}) \le \mathcal{F}_h(a^{n+1,*}, b^{n+1,*}, c^{n+1,*}).$$

A combination of (2.7) and (2.10) results in

$$(2.11) \qquad \mathcal{F}_h(a^{n+1}, b^{n+1}, c^{n+1}) \le \mathcal{F}_h(a^n, b^n, c^n).$$

Therefore, we arrive at the following theoretical result for the operator splitting scheme.

THEOREM 2.1 ([37]). *Given a^n, b^n, c^n, with $a^n_{i,j,k}, b^n_{i,j,k}, c^n_{i,j,k} > 0 \;\forall\, 1 \le i,j,k \le N$, there exists a unique solution a^{n+1}, b^{n+1}, c^{n+1}, with discrete periodic or Neumann boundary conditions, for the operator splitting numerical scheme ((2.5) combined with (2.8)). The pointwise positivity is ensured: $0 < a^{n+1}_{i,j,k}, b^{n+1}_{i,j,k}, c^{n+1}_{i,j,k} \;\forall\, 1 \le i,j,k \le N$. In addition, we have the energy dissipation estimate: $\mathcal{F}_h(a^{n+1}, b^{n+1}, c^{n+1}) \le \mathcal{F}_h(a^n, b^n, c^n)$, so that $\mathcal{F}_h(a^n, b^n, c^n) \le \mathcal{F}_h(a^0, b^0, c^0)$.*

3. Optimal rate convergence analysis and error estimate. Numerical results in [37] indicate that the operator splitting scheme can achieve first-order accuracy in time and second-order accuracy in space. However, a theoretical justification of the convergence analysis turns out to be a challenging subject, due to the nonlinear and singular nature of the reaction part. The main theoretical result of this paper is the following convergence theorem.

THEOREM 3.1. *Given positive initial data $a_0, b_0, c_0 \in C^4_{\mathrm{per}}(\Omega)$, suppose the exact solution for the reaction-diffusion system (1.1), denoted (a_e, b_e, c_e), is of regularity class $[\mathcal{R}]^3$, where*

$$(3.1) \qquad \mathcal{R} := C^2\left(0, T; C_{\mathrm{per}}(\Omega)\right) \cap C^1\left(0, T; C^1_{\mathrm{per}}(\Omega)\right) \cap L^\infty\left(0, T; C^4_{\mathrm{per}}(\Omega)\right).$$

Then, provided Δt and h are sufficiently small, we have

$$(3.2) \qquad \|a^n_e - a^n\|_\infty + \|b^n_e - b^n\|_\infty + \|c^n_e - c^n\|_\infty \le C(\Delta t + h^2)$$

for all positive integers n, such that $t_n = n\Delta t \le T$, where $C > 0$ is independent of Δt and h, a^n_e, b^n_e, and c^n_e are exact solutions at t^n.

As a consequence of the regularity assumption (3.1), the following bound is available for the exact solution:

$$(3.3) \qquad \|\mathbf{u}_e\|_{C^2(0,T;C^0)} \le C_0, \quad \|\mathbf{u}_e(\cdot, t)\|_{C^4(\Omega)} \le C_0 \;\;\forall t \ge 0.$$

In particular, there exists a constant C_0 such that

(3.4)
$$\sup_{\mathbf{x},t} \max\{|a_e(\mathbf{x},t)| + |\partial_t a_e(\mathbf{x},t)|, |b_e(\mathbf{x},t)| + |\partial_t b_e(\mathbf{x},t)|, |c_e(\mathbf{x},t)| + |\partial_t c_e(\mathbf{x},t)|\} \le C_0.$$

In addition, the following separation property is also assumed for the exact solutions:

(3.5)
$$a_e(\mathbf{x},t), \, b_e(\mathbf{x},t), \, c_e(\mathbf{x},t) \ge \epsilon_0 \quad \exists \epsilon_0 > 0.$$

In fact, this assumption is necessary to ensure the regularity requirement (3.1) for the exact solutions, because of the $\ln \frac{a}{a^\infty}$, $\ln \frac{b}{b^\infty}$, $\ln \frac{c}{c^\infty}$ terms appearing in the free energy. In fact, such a separation property has already been established for the 2-D Cahn–Hilliard equation with Flory–Huggins energy potential [1, 11, 22, 24, 43], and this property is expected to hold for the reaction-diffusion system (1.1) in the energetic variational formulation.

3.1. Consistency analysis for the operator splitting scheme. We first perform a consistency analysis [3] for the operator splitting scheme. Given $\mathbf{u}_e^n = (a_e^n, b_e^n, c_e^n)^T$, with the regularity assumption (3.1) and separation assumption (3.5) satisfied, we introduce $\mathbf{u}_e^{n+1,*} = (a_e^{n+1,*}, b_e^{n+1,*}, c_e^{n+1,*})^T$ as the exact update of the first stage equation: $\partial_t \mathbf{u} = \mathcal{A}\mathbf{u}$, over the time interval (t^n, t^{n+1}), with initial data $\mathbf{u}_e^n$. In other words, $\mathbf{u}_e^{n+1,*} = (a_e^{n+1,*}, b_e^{n+1,*}, c_e^{n+1,*})^T$ is the exact solution at $t = t^{n+1}$ for the reaction-only equation

(3.6)
$$\begin{cases} \partial_t \mathbf{u} = \mathcal{A}\mathbf{u}, \\ \mathbf{u}(\mathbf{x}, t^n) = \mathbf{u}_e^n(\mathbf{x}). \end{cases}$$

Meanwhile, as mentioned in the previous section, (3.6) can be reformulated as an equation of the reaction trajectory $R_e(\mathbf{x}, t)$ over the time interval (t^n, t^{n+1}), since

$$a_e(\mathbf{x},t) = a_e^n(\mathbf{x}) - R_e(\mathbf{x},t), \,\, b_e(\mathbf{x},t) = b_e^n(\boldsymbol{x}) - R_e(\mathbf{x},t), \,\, c_e(\mathbf{x},t) = c_e^n(\boldsymbol{x}) + R_e(\mathbf{x},t).$$

The equation for R_e is given by

(3.7)
$$\begin{cases} \ln\left(\frac{\partial_t R_e}{c_e^n + R_e} + 1\right) = \ln\left(\frac{a_e^n - R_e}{a^\infty}\right) + \ln\left(\frac{b_e^n - R_e}{b^\infty}\right) - \ln\left(\frac{c_e^n + R_e}{c^\infty}\right), \\ R_e(\cdot, t^n) \equiv 0. \end{cases}$$

Moreover, we have

(3.8)
$$a_e^{n+1,*} = a_e^n - R_e^{n+1}, \quad b_e^{n+1,*} = b_e^n - R_e^{n+1}, \quad c_e^{n+1,*} = c_e^n + R_e^{n+1}.$$

By a careful Taylor expansion in time, one can show that the exact equation (3.7) can be approximated by the temporal discretization (2.5) with $O(\Delta t)$ accuracy:

(3.9)
$$\begin{aligned} \ln\left(\frac{R_e^{n+1} - R_e^n}{(c_e^n + R_e^n)\Delta t} + 1\right) = \,\,& \ln\left(\frac{a_e^n - R_e^{n+1}}{a^\infty}\right) + \ln\left(\frac{b_e^n - R_e^{n+1}}{b^\infty}\right) \\ & - \ln\left(\frac{c_e^n + R_e^{n+1}}{c^\infty}\right) + \tau_0^{n+1}, \end{aligned}$$

where $R_e^n \equiv 0$ and $|\tau_0^{n+1}| \le C\Delta t$ is the local truncation error at a pointwise level. The consistency estimate (3.9) could be rewritten as the following equation after an exponential transform:

(3.10)
$$\frac{R_e^{n+1} - R_e^n}{(c_e^n + R_e^n)\Delta t} = \frac{(a_e^n - R_e^{n+1})(b_e^n - R_e^{n+1})}{c_e^n + R_e^{n+1}} - 1 + \tau_1^{n+1},$$

where $|\tau_1^{n+1}| \le C\Delta t$ due to the fact that $e^{\tau_0^{n+1}} - 1 = O(\Delta t)$ for $\tau_0^{n+1} = O(\Delta t)$.

In the second stage, given $\mathbf{u}_e^{n+1,*} = (a_e^{n+1,*}, b_e^{n+1,*}, c_e^{n+1,*})^T$, we denote the exact update by $\mathbf{u}_e^{n+1,**} = (a_e^{n+1,**}, b_e^{n+1,**}, c_e^{n+1,**})^T$, i.e., $\mathbf{u}_e^{n+1,**}$ is the exact solution for the linear diffusion equation

$$(3.11) \qquad \begin{aligned} \partial_t \mathbf{u} = \mathcal{B}\mathbf{u} = \nabla \cdot (\mathcal{D}(\mathbf{x})\nabla \mathbf{u}), \\ \mathbf{u}(\cdot, t^n) = \mathbf{u}_e^{n+1,*} \end{aligned}$$

at $t = t^{n+1}$. By a careful Taylor expansion associated with the operator splitting $\mathbf{u}_e^{n+1,**} = e^{\mathcal{B}\Delta t} e^{\mathcal{A}\Delta t} \mathbf{u}_e^n$, one can show that

$$(3.12) \qquad \mathbf{u}_e^{n+1,**} - \mathbf{u}_e^{n+1} = O(\Delta t^2).$$

On the other hand, an application of implicit Euler temporal discretization to the diffusion equation system (3.11) implies the consistency estimate

$$(3.13) \qquad \frac{\mathbf{u}_e^{n+1,**} - \mathbf{u}_e^{n+1,*}}{\Delta t} = \nabla \cdot (\mathcal{D}(\mathbf{x})\nabla \mathbf{u}_e^{n+1,**}) + \tau_{2,t}^{n+1,(1)},$$

where $|\tau_{2,t}^{n+1,(1)}| \le C\Delta t$ is the local truncation error. In turn, its combination with (3.12) yields

$$(3.14) \qquad \frac{\mathbf{u}_e^{n+1} - \mathbf{u}_e^{n+1,*}}{\Delta t} = \nabla \cdot (\mathcal{D}(\mathbf{x})\nabla \mathbf{u}_e^{n+1}) + \tau_{2,t}^{n+1},$$

where $|\tau_{2,t}^{n+1}| \le C\Delta t$. Furthermore, the centered difference approximation for $\mathbf{u}_e^{n+1}$ leads to the following truncation error estimate:

$$(3.15) \qquad |\nabla \cdot (\mathcal{D}(\mathbf{x})\nabla \mathbf{u}_e^{n+1}) - \nabla_h \cdot (\mathcal{D}\nabla_h \mathbf{u}_e^{n+1})| \le Ch^2, \quad \text{pointwise on the mesh.}$$

Then we obtain the consistency estimate for the second stage:

$$(3.16) \qquad \frac{\mathbf{u}_e^{n+1} - \mathbf{u}_e^{n+1,*}}{\Delta t} = \nabla_h \cdot (\mathcal{D}\nabla_h \mathbf{u}_e^{n+1}) + \tau_2^{n+1},$$

where $|\tau_2^{n+1}| \le C(\Delta t + h^2)$.

In summary, we have the consistency analysis for the operator splitting scheme,

$$(3.17) \qquad \frac{R_e^{n+1} - R_e^n}{(c_e^n + R_e^n)\Delta t} = \frac{(a_e^n - R_e^{n+1})(b_e^n - R_e^{n+1})}{c_e^n + R_e^{n+1}} - 1 + \tau_1^{n+1}, \quad R_e^n = 0,$$

$$(3.18) \qquad a_e^{n+1,*} = a_e^n - R_e^{n+1}, \quad b_e^{n+1,*} = b_e^n - R_e^{n+1}, \quad c_e^{n+1,*} = c_e^n + R_e^{n+1},$$

$$(3.19) \qquad \frac{\mathbf{u}_e^{n+1} - \mathbf{u}_e^{n+1,*}}{\Delta t} = \nabla_h \cdot (\mathcal{D}\nabla_h \mathbf{u}_e^{n+1}) + \tau_2^{n+1},$$

where

$$(3.20) \qquad |\tau_1^{n+1}| \le C\Delta t \quad \text{and} \quad |\tau_2^{n+1}| \le C(\Delta t + h^2).$$

Of course, the local truncation error is of order $O(\Delta t + h^2)$.

3.2. Error estimate in the first stage. We first perform the error estimate in the reaction stage. Define the pointwise error functions:

(3.21)
$$e_a^k := a_e^k - a^k, \quad e_b^k := b_e^k - b^k, \quad e_c^k := c_e^k - c^k, \quad e_R^k := R_e^k - R^k,$$

$$e_a^{n+1,*} := a_e^{n+1,*} - a^{n+1,*}, \quad e_b^{n+1,*} := b_e^{n+1,*} - b^{n+1,*}, \quad e_c^{n+1,*} := c_e^{n+1,*} - c^{n+1,*}$$

for any $k \geq 0$, $n \geq 0$. The numerical scheme for the reaction stage (2.5) may, of course, be rewritten by an exponential transform,

(3.22)
$$\frac{R^{n+1} - R^n}{(c^n + R^n)\Delta t} = \frac{(a^n - R^{n+1})(b^n - R^{n+1})}{c^n + R^{n+1}} - 1, \quad R^n \equiv 0.$$

Subtracting the rewritten scheme (3.22) from the consistency estimate (3.17) and rearranging terms yields

(3.23)
$$\frac{e_R^{n+1}}{c^n \Delta t} = q_0^{n+1} e_c^n - (q_1^{n+1} + q_2^{n+1} + q_3^{n+1}) e_R^{n+1} + q_1^{n+1} e_a^n + q_2^{n+1} e_b^n - q_3^{n+1} e_c^n + \tau_1^{n+1},$$

where

(3.24)
$$q_0^{n+1} := \frac{R_e^{n+1}}{c_e^n \cdot c^n \Delta t}, \quad q_1^{n+1} := \frac{b^n - R^{n+1}}{c^n + R^{n+1}},$$

$$q_2^{n+1} := \frac{a_e^n - R_e^{n+1}}{c^n + R^{n+1}}, \quad q_3^{n+1} := \frac{(a_e^n - R_e^{n+1})(b_e^n - R_e^{n+1})}{(c^n + R^{n+1})(c_e^n + R_e^{n+1})}.$$

Remark 3.1. We observe that

(3.25)
$$\frac{AB}{C} - \frac{(A + \xi_A)(B + \xi_B)}{C + \xi_B} = \frac{AB\xi_C}{(C + \xi_C)C} - \frac{\xi_A \xi_B}{C + \xi_C} - \frac{A\xi_B + B\xi_A}{C + \xi_C}$$

$$= -\frac{B + \xi_B}{C + \xi_C}\xi_A - \frac{A}{C + \xi_C}\xi_B + \frac{AB}{C(C + \xi_C)}\xi_C.$$

By taking $A = a_e^n - R_e^{n+1}$, $B = b_e^n - R_e^{n+1}$, $C = c_e^n + R_e^{n+1}$, $\xi_A = -e_a^n + e_R^{n+1}$, $\xi_B = -e_b^n + e_R^{n+1}$, and $\xi_C = -e_c^n - e_R^{n+1}$, we can obtain (3.23).

The error evolutionary equation (3.23) could be rewritten as

(3.26)
$$M^{n+1} e_R^{n+1} = q_0^{n+1} e_c^n + (q_1^{n+1} e_a^n + q_2^{n+1} e_b^n - q_3^{n+1} e_c^n) + \tau_1^{n+1},$$

where M^{n+1} is defined by

(3.27)
$$M^{n+1} := \frac{1}{c^n \Delta t} + (q_1^{n+1} + q_2^{n+1} + q_3^{n+1}).$$

To proceed with the nonlinear analysis, we first make the following a priori assumption for the previous time step:

(3.28)
$$\|e_a^n\|_\infty \leq \Delta t^{\frac{1}{2}} + h, \quad \|e_b^n\|_\infty \leq \Delta t^{\frac{1}{2}} + h, \quad \|e_c^n\|_\infty \leq \Delta t^{\frac{1}{2}} + h.$$

Such an a priori assumption will be recovered by the optimal rate convergence analysis at the next time step, as demonstrated later.

A direct consequence of the assumption (3.28) gives the following bound and separation property for the numerical solution at the previous time step:

(3.29)
$$|a^n| \leq |a_e^n| + |e_a^n| \leq C_0 + 1 := C_1, \quad |b^n| \leq C_1, \quad |c^n| \leq C_1,$$

$$a^n \geq a_e^n - |e_a^n| \geq \frac{\epsilon_0}{2}, \quad b^n \geq \frac{\epsilon_0}{2}, \quad c^n \geq \frac{\epsilon_0}{2},$$

provided that

$$\Delta t^{\frac{1}{2}}, \, h \leq \min\left(\frac{\epsilon_0}{4}, \frac{1}{2}\right).$$

Here we have made use of the functional bound (3.3) and the separation property (3.5) for the exact solution.

Due the positivity-preserving property for both the exact solution and the numerical solution (coming from Theorem 2.1), it is obvious that

$$
\begin{aligned}
(3.30) \quad & a_e^n - R_e^{n+1} > 0, \;\; b_e^n - R_e^{n+1} > 0, \;\; c_e^n + R_e^{n+1} > 0, \\
& a^n - R^{n+1} > 0, \;\; b^n - R^{n+1} > 0, \;\; c^n + R^{n+1} > 0,
\end{aligned}
$$

which, in turn, implies that

$$(3.31) \qquad q_1^{n+1} > 0, \quad q_2^{n+1} > 0, \quad q_3^{n+1} > 0.$$

Meanwhile, the $C^2([0,T])$ bound for the exact solution R_e indicates that $\left|\frac{R_e^{n+1}}{\Delta t}\right| \leq C_0$. The separation estimates for the exact and numerical solutions, given by (3.5) and (3.29), respectively, lead to $0 < \frac{1}{c^n \cdot c_e^n} < \frac{4}{\epsilon_0^2}$. In turn, q_0^{n+1} is uniformly bounded by

$$(3.32) \qquad |q_0^{n+1}| \leq \frac{4C_0}{\epsilon_0^2} := C_2.$$

A rough error estimate on $\|e_R^{n+1}\|_\infty \lesssim \Delta t^{1/2} + h$ can be obtained based on the following simple estimates:

$$(3.33) \qquad M^{n+1} \geq \frac{1}{(c^n + R^n)\Delta t} \Longrightarrow 0 < \frac{1}{M^{n+1}} \leq c^n \Delta t \leq C_1 \Delta t,$$

$$(3.34) \qquad M^{n+1} \geq q_1^{n+1} + q_2^{n+1} + q_3^{n+1} \Longrightarrow 0 < \frac{q_1^{n+1} + q_2^{n+1} + q_3^{n+1}}{M^{n+1}} \leq 1,$$

$$(3.35) \qquad \left|\frac{q_0^{n+1}}{M^{n+1}}\right| \leq \left|\frac{C_2}{\frac{1}{c^n \Delta t}}\right| \leq C_2 c^n \Delta t \leq C_2 C_1 \Delta t.$$

Moreover, since $q_1^{n+1} > 0$, $q_2^{n+1} > 0$, $q_3^{n+1} > 0$, it is straightforward to see that

$$
\begin{aligned}
(3.36) \quad \left|\frac{q_1^{n+1} e_a^n + q_2^{n+1} e_b^n - q_3^{n+1} e_c^n}{M^{n+1}}\right| &\leq \frac{q_1^{n+1} + q_2^{n+1} + q_3^{n+1}}{M^{n+1}} \max(|e_a^n|, |e_b^n|, |e_c^n|) \\
&\leq \max(|e_a^n|, |e_b^n|, |e_c^n|).
\end{aligned}
$$

A substitution of (3.33), (3.35), and (3.36) into (3.26) leads to

$$
\begin{aligned}
(3.37) \quad |e_R^{n+1}| &\leq \frac{|q_0^{n+1}|}{M^{n+1}}|e_c^n| + \left|\frac{q_1^{n+1} e_a^n + q_2^{n+1} e_b^n - q_3^{n+1} e_c^n}{M^{n+1}}\right| + \frac{1}{M^{n+1}}|\tau_1^{n+1}| \\
&\leq C_1 C_2 \Delta t |e_c^n| + \max(|e_a^n|, |e_b^n|, |e_c^n|) + C_1 \Delta t |\tau_1^{n+1}|.
\end{aligned}
$$

With the a priori numerical error assumption at the previous time step (3.28), we arrive at a rough error estimate for e_R^{n+1}:

$$(3.38) \quad |e_R^{n+1}| \leq 2(\Delta t^{\frac{1}{2}} + h) + C_1 \Delta t |\tau_1^{n+1}| \leq 2(\Delta t^{\frac{1}{2}} + h) + CC_1 \Delta t^2 \leq 3\Delta t^{\frac{1}{2}} + 2h,$$

provided that $C_1 C_2 \Delta t \leq 1$ and $CC_1 (\Delta t)^{3/2} < 1$. Here the local truncation error estimate $|\tau_1^{n+1}| \leq C\Delta t$ has been used.

The rough error estimate on e_R^{n+1} enables us to refine the estimates on q_i^{n+1}, which is the key to obtaining the error estimate of the desired order. As a result of this rough estimate, the following estimates can be derived:

$$(3.39) \quad c_e^n + R_e^{n+1} \geq \epsilon_0 - C_0 \Delta t \geq \frac{\epsilon_0}{2} \quad (\text{since } |R_e^{n+1}| \leq C_0 \Delta t),$$

$$(3.40) \quad |e_c^n| + |e_R^{n+1}| \leq 4 \Delta t^{\frac{1}{2}} + 3h \leq \min\left(\frac{\epsilon_0}{4}, 1\right) \quad (\text{using } (3.28), (3.38)),$$

$$(3.41) \quad c^n + R^{n+1} \geq c_e^n + R_e^{n+1} - (|e_c^n| + |e_R^{n+1}|) \geq \frac{\epsilon_0}{4},$$

$$(3.42) \quad c^n + R^{n+1} \leq c_e^n + R_e^{n+1} + (|e_c^n| + |e_R^{n+1}|) \leq C_1 + 1,$$

provided that $C_0 \Delta t \leq \frac{\epsilon_0}{2}$ and $4 \Delta t^{\frac{1}{2}} + 3h \leq \min(\frac{\epsilon_0}{4}, 1)$. The same estimate can be made for a and b. Then we obtain

$$(3.43) \quad 0 < q_1^{n+1} = \frac{b^n - R^{n+1}}{c^n + R^{n+1}} \leq \frac{C_1 + 1}{\frac{\epsilon_0}{4}} = 4(C_1 + 1)\epsilon_0^{-1},$$

$$(3.44) \quad 0 < q_2^{n+1} = \frac{a_e^n - R_e^{n+1}}{c^n + R^{n+1}} \leq \frac{C_1}{\frac{\epsilon_0}{4}} = 4C_1 \epsilon_0^{-1},$$

$$(3.45) \quad 0 < q_3^{n+1} = \frac{(a_e^n - R_e^{n+1})(b_e^n - R_e^{n+1})}{(c^n + R^{n+1})(c_e^n + R_e^{n+1})} \leq \frac{C_1^2}{\frac{\epsilon_0^2}{8}} = 8C_1^2 \epsilon_0^{-2},$$

so that the following uniform bound is available:

$$(3.46) \quad 0 < q_1^{n+1} + q_2^{n+1} + q_3^{n+1} \leq C_3 := (8C_1 + 4)\epsilon_0^{-1} + 8C_1^2 \epsilon_0^{-2}.$$

Consequently, we have the refined estimate

$$\left| \frac{q_1^{n+1} e_a^n + q_2^{n+1} e_b^n - q_3^{n+1} e_c^n}{M^{n+1}} \right| \leq \frac{1}{M^{n+1}} (q_1^{n+1} + q_2^{n+1} + q_3^{n+1}) \max(|e_a^n|, |e_b^n|, |e_c^n|)$$

$$(3.47) \quad \leq C_1 C_3 \Delta t \max(|e_a^n|, |e_b^n|, |e_c^n|).$$

Going back to the earlier error estimate (3.37), we arrive at

$$|e_R^{n+1}| \leq \frac{|q_0^{n+1}|}{M^{n+1}} |e_c^n| + \left| \frac{q_1^{n+1} e_a^n + q_2^{n+1} e_b^n - q_3^{n+1} e_c^n}{M^{n+1}} \right| + \frac{1}{M^{n+1}} |\tau_1^{n+1}|$$

$$\leq C_1 C_2 \Delta t |e_c^n| + C_1 C_3 \Delta t \max(|e_a^n|, |e_b^n|, |e_c^n|) + C_1 \Delta t |\tau_1^{n+1}|$$

$$(3.48) \quad \leq 2C_1(C_2 + C_3)\Delta t \max(|e_a^n|, |e_b^n|, |e_c^n|) + C_1 \Delta t |\tau_1^{n+1}|.$$

On the other hand, a difference between the numerical solution (2.6) and the constructed profile (3.18) reveals that

$$(3.49) \quad e_a^{n+1,*} = e_a^n - e_R^{n+1}, \quad e_b^{n+1,*} = e_b^n - e_R^{n+1}, \quad e_c^{n+1,*} = e_c^n + e_R^{n+1}.$$

Then we arrive at the following error estimate in the first stage:

$$(3.50) \quad |e_a^{n+1,*}| \leq |e_a^n| + |e_R^{n+1}| \leq (1 + C_4 \Delta t) \max(|e_a^n|, |e_b^n|, |e_c^n|) + C_1 \Delta t |\tau_1^{n+1}|,$$

$$(3.51) \quad |e_b^{n+1,*}| \leq |e_b^n| + |e_R^{n+1}| \leq (1 + C_4 \Delta t) \max(|e_a^n|, |e_b^n|, |e_c^n|) + C_1 \Delta t |\tau_1^{n+1}|,$$

$$(3.52) \quad |e_c^{n+1,*}| \leq |e_c^n| + |e_R^{n+1}| \leq (1 + C_4 \Delta t) \max(|e_a^n|, |e_b^n|, |e_c^n|) + C_1 \Delta t |\tau_1^{n+1}|,$$

with $C_4 := (1 + M_0)C_1(C_2 + C_3)$. Since the error estimate (3.50)–(3.52) is valid at a pointwise level, the following conclusion is made:

$$(3.53) \quad \begin{aligned} \|e_a^{n+1,*}\|_\infty, \|e_b^{n+1,*}\|_\infty, \|e_c^{n+1,*}\|_\infty \\ \leq (1 + C_4 \Delta t) \max(\|e_a^n\|_\infty, \|e_b^n\|_\infty, \|e_c^n\|_\infty) + C_1 \Delta t \|\tau_1^{n+1}\|_\infty. \end{aligned}$$

Remark 3.2. In the rough error estimate (3.38), we see that the accuracy order is lower than the desired accuracy order. Therefore, such a rough estimate could not be used for a global induction analysis. Instead, the purpose of such an estimate is to establish a uniform $\| \cdot \|_\infty$ bound, so that a discrete separation property becomes available for the numerical solution, as well as its maximum values. With such a property established for the numerical solution, the refined error analysis yields a much sharper estimate than in (3.48). A combination of a rough error estimate and a refined error estimate has been successfully applied to certain nonlinear PDEs with singular terms, such as the PNP system [38], the porous medium equation in the energetic variational formulation [19]. Here we show that such a technique works for the highly nonlinear reaction trajectory equation (1.7).

3.3. Error estimate in the second stage. Now we proceed into the error estimate for the second part. Subtracting the implicit Euler scheme (2.8) from the consistency estimate (3.19) yields

$$(3.54) \qquad \frac{e_a^{n+1} - e_a^{n+1,*}}{\Delta t} = \nabla_h \cdot (D_a \nabla_h e_a^{n+1}) + \tau_{2,a}^{n+1},$$

$$(3.55) \qquad \frac{e_b^{n+1} - e_b^{n+1,*}}{\Delta t} = \nabla_h \cdot (D_b \nabla_h e_b^{n+1}) + \tau_{2,b}^{n+1},$$

$$(3.56) \qquad \frac{e_c^{n+1} - e_c^{n+1,*}}{\Delta t} = \nabla_h \cdot (D_c \nabla_h e_c^{n+1}) + \tau_{2,c}^{n+1},$$

where the local truncation errors $\tau_{2,a}^{n+1}$, $\tau_{2,b}^{n+1}$, and $\tau_{2,c}^{n+1}$ satisfy $|\tau_{2,a}^{n+1}|, |\tau_{2,b}^{n+1}|, |\tau_{2,c}^{n+1}| \leq C(\Delta t + h^2)$ at a pointwise level.

Due to the maximum principle for the discrete elliptic operator in the finite difference setting [29], we have

$$(3.57) \qquad \|e_a^{n+1}\|_\infty \leq \|e_a^{n+1,*}\|_\infty + \Delta t \|\tau_{2,a}^{n+1}\|_\infty,$$

$$(3.58) \qquad \|e_b^{n+1}\|_\infty \leq \|e_b^{n+1,*}\|_\infty + \Delta t \|\tau_{2,b}^{n+1}\|_\infty,$$

$$(3.59) \qquad \|e_c^{n+1}\|_\infty \leq \|e_c^{n+1,*}\|_\infty + \Delta t \|\tau_{2,c}^{n+1}\|_\infty.$$

Indeed, for (3.54) with periodic boundary condition, if e_a^{n+1} takes a maximum value at (i,j,k), we see that

$$(3.60) \qquad \nabla_h \cdot (D_a \nabla_h e_a^{n+1})_{i,j,k} \leq 0$$

by looking at the values of e_a^{n+1} in a neighborhood of (i,j,k), provided that $D_a(\mathbf{x})$ is pointwise nonnegative. Therefore, the inequality

$$(3.61) \qquad (e_a^{n+1})_{i,j,k} \leq (e_a^{n+1,*})_{i,j,k} + \Delta t (\tau_{2,a}^{n+1})_{i,j,k}$$

is valid, which in turn implies that

$$(3.62) \qquad \max_{i,j,k} e_a^{n+1} \leq \max_{i,j,k} e_a^{n+1,*} + \Delta t \max_{i,j,k} \tau_{2,a}^{n+1}.$$

Similarly, we can prove that

$$(3.63) \qquad \min_{i,j,k} e_a^{n+1} \geq \min_{i,j,k} e_a^{n+1,*} - \Delta t \max_{i,j,k} |\tau_{2,a}^{n+1}|.$$

Combining (3.62) and (3.63), we obtain (3.57). Inequalities (3.58) and (3.59) can be proved in the same manner.

3.4. Convergence estimate for the full operator splitting system. A combination of (3.53) and (3.57)–(3.59) reveals that

$$\max(\|e_a^{n+1}\|_\infty, \|e_b^{n+1}\|_\infty, \|e_c^{n+1}\|_\infty) \leq (1 + C_4 \Delta t) \max(\|e_a^n\|_\infty, \|e_b^n\|_\infty, \|e_c^n\|_\infty)$$

$$(3.64) \qquad\qquad + (1 + C_1) \Delta t (\|\tau_1^{n+1}\|_\infty + \|\tau_2^{n+1}\|_\infty).$$

Therefore, an application of a discrete Gronwall inequality leads to the desired convergence estimate

$$(3.65) \qquad \max(\|e_a^{n+1}\|_\infty, \|e_b^{n+1}\|_\infty, \|e_c^{n+1}\|_\infty) \leq C(\Delta t + h^2),$$

based on the truncation error estimates $\|\tau_1^{n+1}\|_\infty \leq C \Delta t$, $\|\tau_2^{n+1}\|_\infty \leq C(\Delta t + h^2)$.

With the $\|\cdot\|_\infty$ error estimate (3.65) at hand, the a priori assumption in (3.28) is satisfied at the next time step t^{n+1}:

$$(3.66) \qquad \|e^{n+1}\|_\infty \leq C(\Delta t + h^2) \leq \Delta t^{\frac{1}{2}} + h,$$

provided Δt and h are sufficiently small. As a result, an induction analysis could be applied. This finishes the proof of Theorem 3.1.

Remark 3.3. There have been many existing works of operator splitting numerical approximation to nonlinear PDEs, such as [12, 13, 62] for reaction-diffusion systems, [5, 7, 40, 51, 52] for the nonlinear Schrödinger equation, [4] for the incompressible magnetohydrodynamics system, [6] for the delay equation, [20] for the nonlinear evolution equation, [21] for the Vlasov-type equation, [31] for a generalized Leland mode, [58, 59] for the "good" Boussinesq equation, [33] for the Allen–Cahn equation, [34] for the molecular beamer epitaxy (MBE) equation, [61] for nonlinear solvation problem, etc. A few convergence estimates have also been reported for gradient flow with polynomial energy potential, such as [34, 59]. The convergence result stated in this article provides a theoretical convergence analysis for an operator splitting scheme for an energy variational formulation with singular energy potential involved.

4. A near-equilibrium dynamics: The linear response regime. In classical chemical kinetics, it is often assumed that the reaction rate is directly proportional to the product of the concentrations of the reactants, known as the *law of mass action*. The reaction rate given by system (1.1), namely, $\pm(ab - c)$, stands for a special example. The law of mass action gives a simple form of the reaction rate in terms of concentration variables; however, the dissipation in terms of R and R_t becomes complicated; see (1.7), in which $\ln\left(1 + \frac{R_t}{c}\right)$ is involved.

For chemical reactions, a few recent works employ the linear response assumption on R to derive a reaction kinetics near the equilibrium [36, 54]. For system (1.5), it is clear that $R_t \approx 0$ near the equilibrium of the chemical reaction. In turn, an application of the Taylor expansion implies that

$$(4.1) \qquad\qquad \ln\left(1 + \frac{R_t}{c}\right) \approx \frac{1}{c} R_t.$$

Hence, one can take the dissipation for the reaction part as $\frac{1}{c}|R_t|^2$ near the chemical equilibrium, which corresponds to the linear response assumption in nonequilibrium thermodynamics [44, 45, 23]. In this case, the reaction-only part takes the form

$$(4.2) \qquad \partial_t a = -c \ln\left(\frac{ab}{c}\right), \quad \partial_t b = -c \ln\left(\frac{ab}{c}\right), \quad \partial_t c = c \ln\left(\frac{ab}{c}\right),$$

and the reaction trajectory R satisfies the equation

$$(4.3) \qquad \frac{1}{c} R_t = \ln\left(\frac{ab}{c}\right) = \ln(a_0 - R) + \ln(b_0 - R) - \ln(c_0 + R) = -\frac{\delta \tilde{\mathcal{F}}}{\delta R},$$

in which $\tilde{\mathcal{F}}(R)$ takes the same form as $\mathcal{F}(a, b, c) = \tilde{\mathcal{F}}(R)$. Notice that if $ab - c \ll c$,

$$(4.4) \qquad R_t = c \ln\left(\frac{ab}{c}\right) = c \ln\left(\frac{ab - c}{c} + 1\right) \approx c \frac{ab - c}{c} = ab - c,$$

which is consistent with the law of mass action. A similar argument was proposed in Onsager's seminal work [44], in which he showed that the law of mass action for the reaction network A $\rightleftharpoons$ B $\rightleftharpoons$ C $\rightleftharpoons$ A satisfies the reciprocal relation near the equilibrium.

In this section, we consider the reaction-diffusion system with the reaction dissipation given by the linear response theory:

$$(4.5) \qquad \begin{cases} \partial_t a = \nabla \cdot (D_a(\mathbf{x}) \nabla a) - c \ln\left(\frac{ab}{c}\right), \\ \partial_t b = \nabla \cdot (D_b(\mathbf{x}) \nabla b) - c \ln\left(\frac{ab}{c}\right), \\ \partial_t c = \nabla \cdot (D_c(\mathbf{x}) \nabla c) + c \ln\left(\frac{ab}{c}\right), \end{cases}$$

subject to a periodic boundary condition and a positive initial data. Here the diffusion part (1.8) has the same dissipation law (1.9) and the energy-dissipation law for the overall system could be formulated as

$$(4.6) \qquad \begin{aligned} \frac{\mathrm{d}}{\mathrm{d}t} \mathcal{F}(a, b, c) = &-\int_\Omega D_a(\mathbf{x}) a |\nabla \mu_A|^2 + D_b(\mathbf{x}) b |\nabla \mu_B|^2 + D_c(\mathbf{x}) c |\nabla \mu_C|^2 \\ &+ \frac{1}{c} |R_t|^2 \mathrm{d}\mathbf{x} \le 0. \end{aligned}$$

The numerical discretization of the reaction part in (1.1) is more challenging than that in (1.8) if one discretizes the concentration variables directly. Meanwhile, it is noticed in (4.3) that the reaction part is an L^2-gradient flow in R. Although the reaction rates in system (4.5) do not obey the law of mass action and the numerical schemes reported in [37] have not covered this system, a similar idea of operator splitting could be efficiently applied to (4.5). In more details, given a^n, b^n, c^n, with $a^n, b^n, c^n > 0$ at each mesh point, the numerical solutions a^{n+1}, b^{n+1} and c^{n+1} are updated via the following two stages. For simplicity of presentation, we take $a^\infty = b^\infty = c^\infty = 1$ throughout this section.

Stage 1. First, we set $R^n \equiv 0$ and solve

$$(4.7) \qquad \frac{1}{c^n} \frac{R^{n+1} - R^n}{\Delta t} = \ln(a^n - R^{n+1}) + \ln(b^n - R^{n+1}) - \ln(c^n + R^{n+1})$$

at each mesh point. Using similar techniques reported in [37], in particular the convexity analysis of the logarithmic energy potential, we are able to prove that there exists a unique solution R^{n+1} such that $a^n - R^{n+1} > 0$, $b^n - R^{n+1} > 0$, and $c^n + R^{n+1} > 0$. Also, the intermediate numerical variables, $(a^{n+1,*}, b^{n+1,*}, c^{n+1,*})$, are denoted as in (2.6), and the energy dissipation property (2.7) can be similarly established.

Stage 2. With the pointwise positive intermediate variables $a^{n+1,*}$, $b^{n+1,*}$, $c^{n+1,*}$ we update a^{n+1}, b^{n+1}, and c^{n+1} by the standard implicit Euler scheme (2.8). Again, the positivity and energy stability of the implicit Eulerian scheme has been proved in [37], so that (2.9), (2.10), and (2.11) are valid.

In turn, the following theoretical result could be established for the operator splitting scheme; the technical details are left to interested readers.

THEOREM 4.1. *Given a^n, b^n, c^n, with $a_{i,j,k}^n, b_{i,j,k}^n, c_{i,j,k}^n > 0$ $\forall 1 \le i,j,k \le N$, there exists a unique solution a^{n+1}, b^{n+1}, c^{n+1}, with discrete periodic or Neumann boundary conditions, for the operator splitting numerical scheme ((4.7) combined with (2.8)). The pointwise positivity is ensured: $0 < a_{i,j,k}^{n+1}, b_{i,j,k}^{n+1}, c_{i,j,k}^{n+1}$ $\forall 1 \le i,j,k \le N$. In addition, we have the energy dissipation estimate: $\mathcal{F}_h(a^{n+1}, b^{n+1}, c^{n+1}) \le \mathcal{F}_h(a^n, b^n, c^n)$, so that $\mathcal{F}_h(a^n, b^n, c^n) \le \mathcal{F}_h(a^0, b^0, c^0)$.*

In contrast to the operator splitting scheme (2.5) and (2.8), which corresponds to the law of mass action, the only essential difference is associated with the left-hand side of (4.7), in which the temporal discretization $\ln\left(\frac{R^{n+1}-R^n}{c^n \Delta t} + 1\right)$ is replaced by a simpler form, $\frac{1}{c^n} \frac{R^{n+1}-R^n}{\Delta t}$, because of the linear response approximation. However, the numerical analysis might be more challenging, as a simpler rewritten form (3.22) is no longer available, and a more complicated logarithmic reaction rate has to be kept in the algorithm. Fortunately, the monotonicity analysis for the logarithmic terms is still applicable, and the following convergence analysis could be established.

THEOREM 4.2. *Given positive initial data $a_0, b_0, c_0 \in C_{\mathrm{per}}^4(\Omega)$, suppose the exact solution for the reaction-diffusion system (4.5), denoted by (a_e, b_e, c_e), is of regularity class $[\mathcal{R}]^3$ (with $\mathcal{R}$ given by (3.1)). Then, provided Δt and h are sufficiently small, the following convergence result holds*

$$(4.8) \quad \|a_e^n - a^n\|_\infty + \|b_e^n - b^n\|_\infty + \|c_e^n - c^n\|_\infty \le C(\Delta t + h^2) \quad \forall n > 1, \ t_n = n\Delta t \le T,$$

in which (a^n, b^n, c^n) is the numerical solution given by the operator splitting scheme (4.7) and (2.8). The constant $C > 0$ is independent of Δt and h, a_e^n, b_e^n, and c_e^n are exact solutions at t^n.

4.1. Consistency analysis. The functional bounds (3.3) and (3.4) for the exact solution, as well the separation property (3.5), are still valid.

Given $\mathbf{u}_e^n = (a_e^n, b_e^n, c_e^n)^T$, with the regularity assumption (3.1) and separation assumption (3.5) satisfied, we similarly introduce $\mathbf{u}_e^{n+1,*} = (a_e^{n+1,*}, b_e^{n+1,*}, c_e^{n+1,*})^T$ as the exact solution at $t = t^{n+1}$ for the reaction-only equation (3.6). Again, (3.6) can be reformulated as an equation of the reaction coordinate $R_e(\mathbf{x}, t)$ over the time interval (t^n, t^{n+1}) by the identity (3.7). For the reaction rate determined by the linear response theory, the equation for R_e becomes

$$(4.9) \qquad \begin{cases} \frac{1}{c^n} \partial_t R_e = \ln(a_e^n - R_e) + \ln(b_e^n - R_e) - \ln(c_e^n + R_e), \\ R_e(\cdot, t^n) \equiv 0. \end{cases}$$

Subsequently, an intermediate exact profile is introduced as (3.8). In turn, a careful Taylor expansion in time implies the following temporal discretization (2.5) with $O(\Delta t)$ accuracy:

$$(4.10) \quad \frac{1}{c^n} \frac{R_e^{n+1} - R_e^n}{\Delta t} = \ln(a_e^n - R_e^{n+1}) + \ln(b_e^n - R_e^{n+1}) - \ln(c_e^n + R_e^{n+1}) + \tau_1^{n+1},$$

where $R_e^n \equiv 0$ and $|\tau_1^{n+1}| \leq C\Delta t$ is the local truncation error at a pointwise level.

The consistency analysis in the second stage could be derived in the same way as in (3.11)–(3.16). Then we obtain the consistency analysis for the operator splitting scheme (4.7) and (2.8):

$$(4.11) \quad \frac{1}{c^n}\frac{R_e^{n+1} - R_e^n}{\Delta t} = \ln(a_e^n - R_e^{n+1}) + \ln(b_e^n - R_e^{n+1}) - \ln(c_e^n + R_e^{n+1}) + \tau_1^{n+1},$$

$$(4.12) \quad a_e^{n+1,*} = a_e^n - R_e^{n+1}, \quad b_e^{n+1,*} = b_e^n - R_e^{n+1}, \quad c_e^{n+1,*} = c_e^n + R_e^{n+1},$$

$$(4.13) \quad \frac{\mathbf{u}_e^{n+1} - \mathbf{u}_e^{n+1,*}}{\Delta t} = \nabla_h \cdot (\mathcal{D}\nabla_h \mathbf{u}_e^{n+1}) + \tau_2^{n+1},$$

with $|\tau_1^{n+1}| \leq C\Delta t$, and $|\tau_2^{n+1}| \leq C(\Delta t + h^2)$.

4.2. Error estimate in the reaction stage. The pointwise error functions are defined as (3.21). Of course, a difference between the reaction stage algorithm (4.7) and the consistency estimate (4.11) and rearranging terms yields

$$(4.14) \quad \frac{e_R^{n+1}}{c^n\Delta t} = q_0^{n+1}e_c^n - (q_a^{n+1} + q_b^{n+1} + q_c^{n+1})e_R^{n+1} + q_a^{n+1}e_a^n + q_b^{n+1}e_b^n - q_c^{n+1}e_c^n + \tau_1^{n+1},$$

$$(4.15) \quad q_0^{n+1} = \frac{R_e^{n+1}}{c_e^n \cdot c^n\Delta t}, \quad , q_a^{n+1} = \frac{1}{\xi_a^{n+1}}, \quad q_a^{n+1} = \frac{1}{\xi_b^{n+1}}, \quad q_c^{n+1} = \frac{1}{\xi_c^{n+1}},$$

$$\xi_a^{n+1} \text{ is between } a^n - R^{n+1} \text{ and } a_e^n - R_e^{n+1},$$

$$\xi_b^{n+1} \text{ is between } b^n - R^{n+1} \text{ and } b_e^n - R_e^{n+1},$$

$$\xi_c^{n+1} \text{ is between } c^n + R^{n+1} \text{ and } c_e^n + R_e^{n+1},$$

in which the intermediate value theorem has been applied. Furthermore, this error evolutionary equation could be rewritten as

$$(4.16) \quad M^{n+1}e_R^{n+1} = q_0^{n+1}e_c^n + (q_a^{n+1}e_a^n + q_b^{n+1}e_b^n - q_c^{n+1}e_c^n) + \tau_1^{n+1},$$

$$(4.17) \quad M^{n+1} := \frac{1}{c^n\Delta t} + (q_a^{n+1} + q_b^{n+1} + q_c^{n+1}).$$

Similar to the nonlinear analysis presented in section 3, we make the a priori assumption (3.28) for the previous time step, which will be recovered by the optimal rate convergence analysis at the next time step. In turn, the maximum norm bound (3.29), as well as the separation property for the numerical solution at the previous time step, becomes a direct consequence of the a priori assumption (3.28). Recalling the positivity-preserving property for both the exact solution and the numerical solution (coming from Theorem 4.1), the pointwise positivity inequality (3.30) is available. By the representation formula (4.15) for q_a^{n+1}, q_b^{n+1}, and q_c^{n+1}, we see that

$$(4.18) \quad q_a^{n+1} > 0, \quad q_c^{n+1} > 0, \quad q_c^{n+1} > 0.$$

Similarly, the uniform bound (3.32) for $|q_0^{n+1}|$ is still valid. Therefore, a rough error estimate on $\|e_R^{n+1}\|_\infty \lesssim \Delta t^{1/2} + h$ becomes available. Indeed, it is easy to show that

$$(4.19) \quad M^{n+1} \geq \frac{1}{c^n\Delta t} \implies 0 < \frac{1}{M^{n+1}} \leq c^n\Delta t \leq C_1\Delta t,$$

$$(4.20) \quad M^{n+1} \geq q_a^{n+1} + q_b^{n+1} + q_c^{n+1} \implies 0 < \frac{q_a^{n+1} + q_b^{n+1} + q_c^{n+1}}{M^{n+1}} \leq 1,$$

where C_1 is a bound for the numerical solution. Its combination with the fact that $q_1^{n+1} > 0$, $q_2^{n+1} > 0$, $q_3^{n+1} > 0$ leads to

$$\left| \frac{q_a^{n+1} e_a^n + q_b^{n+1} e_b^n - q_c^{n+1} e_c^n}{M^{n+1}} \right| \leq \frac{q_a^{n+1} + q_b^{n+1} + q_c^{n+1}}{M^{n+1}} \max(|e_a^n|, |e_b^n|, |e_c^n|)$$

$$(4.21) \qquad\qquad\qquad \leq \max(|e_a^n|, |e_b^n|, |e_c^n|).$$

In turn, a substitution of (4.19) and (4.21) into (4.16) gives

$$|e_R^{n+1}| \leq \frac{|q_0^{n+1}|}{M^{n+1}} |e_c^n| + \left| \frac{q_a^{n+1} e_a^n + q_b^{n+1} e_b^n - q_c^{n+1} e_c^n}{M^{n+1}} \right| + \frac{1}{M^{n+1}} |\tau_1^{n+1}|$$

$$(4.22) \qquad \leq C_1 C_2 \Delta t |e_c^n| + \max(|e_a^n|, |e_b^n|, |e_c^n|) + C_1 \Delta t |\tau_0^{n+1}|.$$

Again, with the a priori numerical error assumption at the previous time step (3.28), a rough error estimate becomes available for e_R^{n+1}:

$$(4.23) \quad |e_R^{n+1}| \leq 2(\Delta t^{\frac{1}{2}} + h) + C_1 \Delta t |\tau_1^{n+1}| \leq 2(\Delta t^{\frac{1}{2}} + h) + CC_1 \Delta t^2 \leq 3\Delta t^{\frac{1}{2}} + 2h,$$

provided that $C_1 C_2 \Delta t \leq 1$ and $CC_1 (\Delta t)^{3/2} < 1$, with the local truncation error estimate $|\tau_1^{n+1}| \leq C\Delta t$ being used.

The rough error estimate on e_R^{n+1} enables us to refine the estimates on q_i^{n+1}. The bound inequalities (3.39)–(3.42) are still valid, and we are able to obtain

$$(4.24) \quad 0 < q_c^{n+1} = \frac{1}{\xi_c} \leq \max\left(\frac{1}{c_e^n + R_e^{n+1}}, \frac{1}{c^n + R^{n+1}} \right) \leq 4\epsilon_0^{-1} \text{ (by (3.39), (3.41))},$$

provided that Δt and h are sufficiently small, in which the representation (4.15) has been applied. Similar estimates can be made for a and b:

$$(4.25) \qquad 0 < q_a^{n+1} = \frac{1}{\xi_a} \leq \max\left(\frac{1}{a_e^n - R_e^{n+1}}, \frac{1}{a^n - R^{n+1}} \right) \leq 4\epsilon_0^{-1},$$

$$(4.26) \qquad 0 < q_b^{n+1} = \frac{1}{\xi_b} \leq \max\left(\frac{1}{b_e^n - R_e^{n+1}}, \frac{1}{b^n - R^{n+1}} \right) \leq 4\epsilon_0^{-1},$$

so that the following uniform bound is available:

$$(4.27) \qquad\qquad 0 < q_a^{n+1} + q_b^{n+1} + q_c^{n+1} \leq C_3 := 12\epsilon_0^{-1}.$$

As a result, the following refined estimate could be derived:

$$\left| \frac{q_a^{n+1} e_a^n + q_b^{n+1} e_b^n - q_c^{n+1} e_c^n}{M^{n+1}} \right| \leq \frac{1}{M^{n+1}} (q_a^{n+1} + q_b^{n+1} + q_c^{n+1}) \max(|e_a^n|, |e_b^n|, |e_c^n|)$$

$$(4.28) \qquad\qquad\qquad \leq C_1 C_3 \Delta t \max(|e_a^n|, |e_b^n|, |e_c^n|).$$

Going back to the earlier error estimate (4.22), we get

$$|e_R^{n+1}| \leq \frac{|q_0^{n+1}|}{M^{n+1}} |e_c^n| + \left| \frac{q_a^{n+1} e_a^n + q_b^{n+1} e_b^n - q_c^{n+1} e_c^n}{M^{n+1}} \right| + \frac{1}{M^{n+1}} |\tau_1^{n+1}|$$

$$\leq C_1 C_2 \Delta t |e_c^n| + C_1 C_3 \Delta t \max(|e_a^n|, |e_b^n|, |e_c^n|) + C_1 \Delta t |\tau_1^{n+1}|$$

$$(4.29) \qquad \leq C_1 (C_2 + C_3) \Delta t \max(|e_a^n|, |e_b^n|, |e_c^n|) + C_1 \Delta t |\tau_1^{n+1}|.$$

Meanwhile, the intermediate error decomposition formula (3.49) is still valid, so that the following error estimate could be derived in the reaction stage:

$$(4.30) \quad |e_a^{n+1,*}| \leq |e_a^n| + |e_R^{n+1}| \leq (1 + \tilde{C}_3 \Delta t) \max(|e_a^n|, |e_b^n|, |e_c^n|) + \Delta t |\tau_1^{n+1}|,$$

$$(4.31) \quad |e_b^{n+1,*}| \leq |e_b^n| + |e_R^{n+1}| \leq (1 + \tilde{C}_3 \Delta t) \max(|e_a^n|, |e_b^n|, |e_c^n|) + \Delta t |\tau_1^{n+1}|,$$

$$(4.32) \quad |e_c^{n+1,*}| \leq |e_c^n| + |e_R^{n+1}| \leq (1 + \tilde{C}_3 \Delta t) \max(|e_a^n|, |e_b^n|, |e_c^n|) + \Delta t |\tau_1^{n+1}|,$$

with $\tilde{C}_3 := C_1(C_2 + C_3)$. This in turn implies that

$$(4.33) \quad \begin{aligned} & \|e_a^{n+1,*}\|_\infty, \ \|e_b^{n+1,*}\|_\infty, \ \|e_c^{n+1,*}\|_\infty \\ & \leq (1 + \tilde{C}_3 \Delta t) \max(\|e_a^n\|_\infty, \|e_b^n\|_\infty, \|e_c^n\|_\infty) + \Delta t \|\tau_1^{n+1}\|_\infty. \end{aligned}$$

Remark 4.1. The numerical schemes reported in [37] are focused on the reaction rate determined by the law of mass action, so that the reaction-diffusion system (4.5) and the numerical algorithm (4.7) (for the reaction stage, in terms of reaction trajectory) have not been covered in the existing reference. Meanwhile, a similar idea of operator splitting is applicable, and the novel techniques of rough/refined error estimates, as reported in subsection 3.2, could be very effectively extended to analyze the proposed method (4.7). Although the reaction rates take a more complicated form than the ones given by the law of mass action, the monotone property of the singular logarithmic terms still persist, which in turn brings great convenience to ensuring the pointwise positivity of the coefficient functions q_a^{n+1}, q_b^{n+1}, and q_c^{n+1} and deriving a rough error estimate (4.23) for e_R^{n+1}. Subsequently, this rough error estimate results in more accurate bounds, (4.24)–(4.26), for the coefficient functions, so that a more refined error estimate (4.29) becomes a direct consequence. In general, the numerical discretization approach and novel techniques of rough/refined error estimates reported in subsection 3.2 could be applied to any reaction-diffusion system with the reaction trajectory formulated as

$$(4.34) \quad \Gamma(R, R_t) = -\frac{\delta \tilde{\mathcal{F}}}{\delta R},$$

in which $\tilde{\mathcal{F}}(R)$ is a singular and convex energy potential in terms of R, and $\Gamma(R, R_t)$ is a monotone function of R_t. The technical details are left to interested readers.

4.3. Convergence estimate for the full operator splitting scheme (4.7) and (2.8). The numerical error functions in the diffusion stage satisfy the same evolutionary equations (3.54)–(3.56) (by subtracting the implicit Euler method (2.8) from the consistency estimate (4.13)). In turn, an application of discrete maximum principle gives the same $\|\cdot\|_\infty$ estimates (3.57)–(3.59).

A combination of (4.33) and (3.57)–(3.59) gives

$$(4.35) \quad \begin{aligned} \max(\|e_a^{n+1}\|_\infty, \|e_b^{n+1}\|_\infty, \|e_c^{n+1}\|_\infty) & \leq (1 + \tilde{C}_3 \Delta t) \max(\|e_a^n\|_\infty, \|e_b^n\|_\infty, \|e_c^n\|_\infty) \\ & \quad + \Delta t (\|\tau_0^{n+1}\|_\infty + \|\tau_2^{n+1}\|_\infty). \end{aligned}$$

Therefore, an application of a discrete Gronwall inequality leads to the desired convergence estimate

$$(4.36) \quad \max(\|e_a^{n+1}\|_\infty, \|e_b^{n+1}\|_\infty, \|e_c^{n+1}\|_\infty) \leq C(\Delta t + h^2),$$

based on the truncation error estimates $\|\tau_0^{n+1}\|_\infty \leq C\Delta t$, $\|\tau_2^{n+1}\|_\infty \leq C(\Delta t + h^2)$. Subsequently, the a priori assumption in (3.28) is satisfied at the next time step t^{n+1}, in the same way as in (3.66), provided Δt and h are sufficiently small. Therefore, an induction analysis could be applied. This finishes the proof of Theorem 4.2.

5. Numerical test. In this section, we present a 2D numerical example for (1.1). The computational domain is taken as $\Omega = (-1, 1)^2$, and the initial condition is set as

(5.1)

$$
\begin{cases}
a_0(x, y) = \frac{1}{2}(-\tanh(\frac{\sqrt{x^2+y^2}-0.2}{0.1}) + 1) + 0.01; \\
b_0(x, y) = \frac{1}{2}(\tanh(\frac{\sqrt{x^2+y^2}-0.2}{0.1}) + 1) + 0.01; \\
c_0(x, y) = \frac{1}{4}\tanh(\frac{\sqrt{x^2+(y-0.2)^2}-0.2}{0.1} + 1) + \frac{1}{4}\tanh(\frac{\sqrt{x^2+(y+0.2)^2}-0.2}{0.1} + 1) + 0.01.
\end{cases}
$$

The diffusion coefficients are given by $D_a \equiv 0.05$, $D_b \equiv 1$, and $D_c \equiv 0.1$. The initial condition and numerical solutions at different time instants are displayed in Figure 5.1.
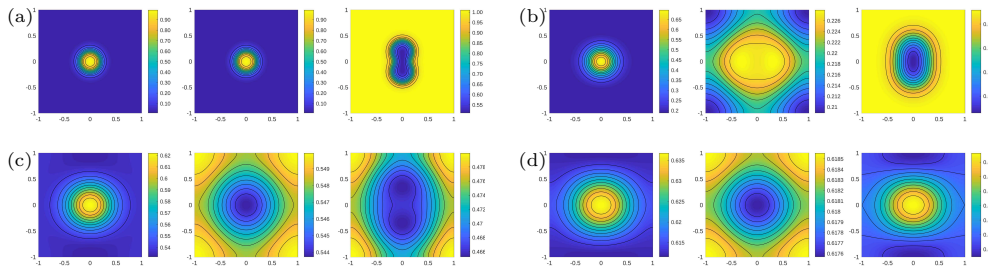

FIG. 5.1. (a)–(d): *Numerical results for the reaction-diffusion system* (1.1) *with* $D_a \equiv 0.05$, $D_b \equiv 1$, $D_c \equiv 0.1$, *and the initial condition* (5.1): (a) $t = 0$, (b) $t = 0.2$, (c) $t = 1$, *and* (d) $t = 2$.

In addition, we look at the numerical error at $T = 0.2$, before the system reaches the constant steady state. Since the analytical solution is not available, we use the numerical solution with $h = 1/200$ and $\Delta t = 1/1600$ as the reference solution in the accuracy test for the temporal numerical errors. Moreover, we fix the spatial resolution as $h = \frac{1}{200}$ for the temporal accuracy test, so that the spatial numerical error is negligible. Table 5.1 displays the $\|\cdot\|_\infty$ numerical errors at $T = 0.2$ with a sequence of time step sizes: $\Delta t = \frac{1}{25}, \frac{1}{50}, \frac{1}{100}, \frac{1}{200}$, and $\frac{1}{400}$. This result indicates a clear first-order accuracy in time.

TABLE 5.1
Numerical errors, order of accuracy for numerical simulations of (1.1) *with* $D_a = 0.05$, $D_b = 1$, $D_c = 0.1$, *and initial condition* (5.1) *at* $T = 0.2$. *The numerical solution with* $h = 1/200$ *and* $\Delta t = 1/1600$ *is taken as the reference solution.*

Δt	h	$\|e_a\|_\infty$	Order	$\|e_b\|_\infty$	Order	$\|e_c\|_\infty$	Order
1/25	1/200	9.5498e-3		1.2498e-2		7.1119e-3	
1/50	1/200	4.8519e-3	0.9769	5.8081e-3	1.1056	3.5450e-3	1.0044
1/100	1/200	2.3840e-3	1.0252	2.7387e-3	1.0846	1.7314e-3	1.0338
1/200	1/200	1.1208e-3	1.0889	1.2629e-3	1.1168	8.1173e-4	1.0929
1/400	1/200	4.8213-4	1.2170	5.3817e-4	1.2306	3.4862e-4	1.2193

To test the spatial accuracy of the operator scheme for this example, we perform the computations on a sequence of mesh resolutions, $h = \frac{1}{20}, \frac{1}{30}, \frac{1}{40}, \frac{1}{50}, \frac{1}{60}$, and the time step size is set as $\Delta t = h^2$ to eliminate the affect of temporal errors. Since an analytical form of the exact solution is not available, we compute the ℓ^∞ differences between numerical solutions with consecutive spatial resolutions, h_{j-1}, h_j, and h_{j+1}, in the Cauchy convergence test. Since we expect the numerical scheme preserves a

second-order spatial accuracy, we can compute the quantity

$$\frac{\ln\left(\frac{1}{A^*}\cdot\frac{\|u_{h_{j-1}}-u_{h_j}\|_\infty}{\|u_{h_j}-u_{h_{j+1}}\|_\infty}\right)}{\ln\frac{h_{j-1}}{h_j}},\quad A^*=\frac{1-\frac{h_j^2}{h_{j-1}^2}}{1-\frac{h_{j+1}^2}{h_j^2}}\quad\text{for }h_{j-1}>h_j>h_{j+1}$$

to check the convergence order [38]. As demonstrated in Table 5.2, an almost perfect second-order spatial convergence rate for the proposed operator splitting scheme is observed.

TABLE 5.2

The ℓ^∞ differences and convergence order for the numerical solutions of a, b, and c at $T = 0.2$. Various mesh resolutions are used: $h_1 = \frac{1}{20}$, $h_2 = \frac{1}{30}$, $h_3 = \frac{1}{40}$, $h_4 = \frac{1}{50}$, $h_5 = \frac{1}{60}$; and the time step size is taken as $\Delta t = h^2$.

—	$\psi = a$	Order	$\psi = b$	Order	$\psi = c$	Order
$\|\psi_{h_1} - \psi_{h_2}\|_\infty$	2.0358e-3	-	4.1584e-4	-	7.6602e-4	-
$\|\psi_{h_2} - \psi_{h_3}\|_\infty$	7.1819e-4	1.9805	1.4459e-4	2.0162	2.6167e-4	2.0599
$\|\psi_{h_3} - \psi_{h_4}\|_\infty$	3.3291e-4	1.9949	6.6751e-5	2.0090	1.2073e-4	2.0111
$\|\psi_{h_3} - \psi_{h_4}\|_\infty$	1.8086e-4	1.9995	3.6211e-5	2.0060	6.5512e-5	2.0048

6. Concluding remarks. A detailed convergence analysis and error estimate have been presented for the variational operator splitting scheme for the reaction-diffusion system (1.1), which satisfies the detailed balance condition. The operator splitting scheme is based on an energetic variational formulation, in which the equation of the reaction trajectory R is introduced in the reaction stage, and both the reaction and diffusion stages dissipate the same discrete free energy [37].

To overcome a well-known difficulty associated with the implicit treatment of the highly nonlinear and singular logarithmic terms, we make use of the convex nature of these nonlinear terms. A combination of rough error estimate and refined error estimate leads to a desired bound of the numerical error at the reaction stage, in the discrete $\|\cdot\|_\infty$ norm. In addition, a discrete maximum principle yields the evolution bound of the numerical error function at the diffusion stage. As a result, a combination of the numerical error analysis at different stages and the consistency estimate for the operator splitting yields the desired convergence estimate for the full reaction-diffusion system in the discrete $\|\cdot\|_\infty$ norm, provided that the exact solutions are sufficiently smooth, and Δt and h are sufficiently small. It is straightforward to extend the analysis to other reaction-diffusion systems with detailed balance [54].

REFERENCES

[1] H. ABELS AND M. WILKE, *Convergence to equilibrium for the Cahn-Hilliard equation with a logarithmic free energy*, Nonlinear Anal., 67 (2007), pp. 3176–3193.

[2] D. F. ANDERSON, G. CRACIUN, M. GOPALKRISHNAN, AND C. WIUF, *Lyapunov functions, stationary distributions, and non-equilibrium potential for reaction networks*, Bull. Math. Biol., 77 (2015), pp. 1744–1767.

[3] D. N. ARNOLD, *Stability, consistency, and convergence of numerical discretizations*, in Encyclopedia of Applied and Computational Mathematics, B. Engquist, ed., Springer, Berlin, Heidelberg, pp. 1358–1364, https://doi.org/10.1007/978-3-540-70529-1_407.

[4] S. BADIA, R. PLANAS, AND J. V. GUTIÉRREZ-SANTACREU, *Unconditionally stable operator splitting algorithms for the incompressible magnetohydrodynamics system discretized by a stabilized finite element formulation based on projections*, Internat. J. Numer. Methods Engrg., 93 (2013), pp. 302–328.

[5] W. BAO, S. JIN, AND P. MARKOWICH, *On time-splitting spectral approximations for the Schrödinger equation in the semiclassical regime*, J. Comput. Phys., 175 (2002), pp. 487–524.

[6] A. BÁTKAI, P. CSOMÓS, AND B. FARKAS, *Operator splitting for nonautonomous delay equations*, Comput. Math. Appl., 65 (2013), pp. 315–324.

[7] C. BESSE, B. BIDÉGARAY, AND S. DESCOMBES, *Order estimates in time of splitting methods for the nonlinear Schrödinger equation*, SIAM J. Numer. Anal., 40 (2002), pp. 26–40, https://doi.org/10.1137/S0036142900381497.

[8] W. CHEN, C. WANG, X. WANG, AND S. WISE, *Positivity-preserving, energy stable numerical schemes for the Cahn-Hilliard equation with logarithmic potential*, J. Comput. Phys. X, 3 (2019), 100031.

[9] M. CHIPOT, D. KINDERLEHRER, AND M. KOWALCZYK, *A variational principle for molecular motors*, Meccanica, 38 (2003), pp. 505–518.

[10] T. DE DONDER, *L'affinité*, Acad. Roy. Belg. Cl. Sci. Mém. Collect. 8, 9 (1927), pp. 1–94.

[11] A. DEBUSSCHE AND L. DETTORI, *On the Cahn-Hilliard equation with a logarithmic free energy*, Nonlinear Anal., 24 (1995), pp. 1491–1514.

[12] S. DESCOMBES, *Convergence of a splitting method of high order for reaction-diffusion systems*, Math. Comp., 70 (2001), pp. 1481–1501.

[13] S. DESCOMBES AND M. MASSOT, *Operator splitting for nonlinear reaction-diffusion systems with an entropic structure: Singular perturbation and order reduction*, Numer. Math., 97 (2004), pp. 667–698.

[14] L. DESVILLETTES AND K. FELLNER, *Exponential decay toward equilibrium via entropy methods for reaction–diffusion equations*, J. Math. Anal. Appl., 319 (2006), pp. 157–176.

[15] L. DESVILLETTES, K. FELLNER, AND B. Q. TANG, *Trend to equilibrium for reaction-diffusion systems arising from complex balanced chemical reaction networks*, SIAM J. Math. Anal., 49 (2017), pp. 2666–2709, https://doi.org/10.1137/16M1073935.

[16] L. DONG, C. WANG, S. WISE, AND Z. ZHANG, *A positivity-preserving, energy stable scheme for a ternary Cahn-Hilliard system with the singular interfacial parameters*, J. Comput. Phys., 442 (2021), 110451.

[17] L. DONG, C. WANG, H. ZHANG, AND Z. ZHANG, *A positivity-preserving, energy stable and convergent numerical scheme for the Cahn-Hilliard equation with a Flory-Huggins-deGennes energy*, Commun. Math. Sci., 17 (2019), pp. 921–939.

[18] L. DONG, C. WANG, H. ZHANG, AND Z. ZHANG, *A positivity-preserving second-order BDF scheme for the Cahn-Hilliard equation with variable interfacial parameters*, Commun. Comput. Phys., 28 (2020), pp. 967–998.

[19] C. DUAN, C. LIU, C. WANG, AND X. YUE, *Convergence analysis of a numerical scheme for the porous medium equation by an energetic variational approach*, Numer. Math. Theoret. Methods Appl., 13 (2020), pp. 63–80.

[20] L. EINKEMMER AND A. OSTERMANN, *An almost symmetric Strang splitting scheme for nonlinear evolution equations*, Comput. Math. Appl., 67 (2014), pp. 2144–2157.

[21] L. EINKEMMER AND A. OSTERMANN, *Convergence analysis of Strang splitting for Vlasov-type equations*, SIAM J. Numer. Anal., 52 (2014), pp. 140–155, https://doi.org/10.1137/130918599.

[22] C. M. ELLIOTT AND H. GARCKE, *On the Cahn–Hilliard equation with degenerate mobility*, SIAM J. Math. Anal., 27 (1996), pp. 404–423, https://doi.org/10.1137/S0036141094267662.

[23] M.-H. GIGA, A. KIRSHTEIN, AND C. LIU, *Variational Modeling and Complex Fluids*, in Handbook of Mathematical Analysis in Mechanics of Viscous Fluids, Springer, Cham, 2018, pp. 73–113.

[24] A. GIORGINI, M. GRASSELLI, AND A. MIRANVILLE, *The Cahn-Hiliard-Ono equation with singular potential*, Math. Models Methods Appl. Sci., 27 (2017), pp. 2485–2510.

[25] A. GLITZKY AND A. MIELKE, *A gradient structure for systems coupling reaction–diffusion effects in bulk and interfaces*, Z. Angew. Math. Phys., 64 (2013), pp. 29–52.

[26] W. HAO AND C. XUE, *Spatial pattern formation in reaction–diffusion models: A computational approach*, J. Math. Biol., 80 (2020), pp. 521–543.

[27] J. HASKOVEC, S. HITTMEIR, P. MARKOWICH, AND A. MIELKE, *Decay to equilibrium for energy-reaction-diffusion systems*, SIAM J. Math. Anal., 50 (2018), pp. 1037–1075, https://doi.org/10.1137/16M1062065.

[28] A. Hawkins-Daarud, K. G. van der Zee, and J. Tinsley Oden, *Numerical simulation of a thermodynamically consistent four-species tumor growth model*, Int. J. Numer. Methods Biomed. Eng., 28 (2012), pp. 3–24.

[29] E. Isaacson and H. B. Keller, *Analysis of Numerical Methods*, Courier Corporation, 2012.

[30] F. Jülicher, A. Ajdari, and J. Prost, *Modeling molecular motors*, Rev. Modern Phys., 69 (1997), pp. 1269–1282.

[31] M. Koleva and L. Vulkov, *Operator splitting kernel based numerical method for a generalized Leland's model*, J. Comput. Appl. Math., 275 (2015), pp. 294–303.

[32] S. Kondo and T. Miura, *Reaction-diffusion model as a framework for understanding biological pattern formation*, Science, 329 (2010), pp. 1616–1620.

[33] H. G. Lee and J. Y. Lee, *A second order operator splitting method for Allen-Cahn type equations with nonlinear source terms*, Phys. A, 432 (2015), pp. 24–34.

[34] X. Li, Z. Qiao, and H. Zhang, *Convergence of a fast explicit operator splitting method for the epitaxial growth model with slope selection*, SIAM J. Numer. Anal., 55 (2017), pp. 265–285, https://doi.org/10.1137/15M1041122.

[35] M. Liero and A. Mielke, *Gradient structures and geodesic convexity for reaction–diffusion systems*, Philos. Trans. R. Soc. Lond. Ser. A Math. Phys. Eng. Sci., 371 (2013), 20120346.

[36] C. Liu and J.-E. Sulzbach, *Well-posedness for the Reaction-diffusion Equation with Temperature in a Critical Besov Space*, preprint, https://arxiv.org/abs/2101.10419, 2021.

[37] C. Liu, C. Wang, and Y. Wang, *A structure-preserving, operator splitting scheme for reaction-diffusion equations involving the law of mass action*, J. Comput. Phys., 436 (2021), 110253.

[38] C. Liu, C. Wang, S. M. Wise, X. Yue, and S. Zhou, *A positivity-preserving, energy stable and convergent numerical scheme for the Poisson-Nernst-Planck system*, Math. Comp., 90 (2021), pp. 2071–2106.

[39] J.-G. Liu, M. Tang, L. Wang, and Z. Zhou, *An accurate front capturing scheme for tumor growth models with a free boundary limit*, J. Comput. Phys., 364 (2018), pp. 73–94.

[40] C. Lubich, *On splitting methods for Schrödinger-Poisson and cubic nonlinear Schrödinger equations*, Math. Comp., 77 (2008), pp. 2141–2153.

[41] A. Mielke, *A gradient structure for reaction–diffusion systems and for energy-drift-diffusion systems*, Nonlinearity, 24 (2011), pp. 1329–1346.

[42] A. Mielke, *Thermomechanical modeling of energy-reaction-diffusion systems, including bulk-interface interactions*, Discrete Contin. Dyn. Syst. Ser. S, 6 (2013), pp. 479–499.

[43] A. Miranville and S. Zelik, *Robust exponential attractors for Cahn-Hilliard type equations with singular potentials*, Math. Methods Appl. Sci., 27 (2004), pp. 545–582.

[44] L. Onsager, *Reciprocal relations in irreversible processes.* I, Phys. Rev., 37 (1931), pp. 405–426.

[45] L. Onsager, *Reciprocal relations in irreversible processes.* II, Phys. Rev., 38 (1931), pp. 2265–2279.

[46] J. E. Pearson, *Complex patterns in a simple system*, Science, 261 (1993), pp. 189–192.

[47] B. Perthame, F. Quirós, and J. L. Vázquez, *The Hele–Shaw asymptotics for mechanical models of tumor growth*, Arch. Ration. Mech. Anal., 212 (2014), pp. 93–127.

[48] J. Prost, F. Jülicher, and J.-F. Joanny, *Active gel physics*, Nature Phys., 11 (2015), pp. 111–117.

[49] Y. Qian, C. Wang, and S. Zhou, *A positive and energy stable numerical scheme for the Poisson-Nernst-Planck-Cahn-Hilliard equations with steric interactions*, J. Comput. Phys., 426 (2021), p. 109908.

[50] D. Shear, *An analog of the Boltzmann h-theorem (a Liapunov function) for systems of coupled chemical reactions*, J. Theoret. Biol., 16 (1967), pp. 212–228.

[51] J. Shen and Z. Wang, *Error analysis of the Strang time-splitting Laguerre-Hermite/Hermite collocation methods for the Gross-Pitaevskii equation*, Found. Comput. Math., 13 (2013), pp. 99–137.

[52] M. Thalhammer, *Convergence analysis of high-order time-splitting pseudospectral methods for nonlinear Schrödinger equations*, SIAM J. Numer. Anal., 50 (2012), pp. 3231–3258, https://doi.org/10.1137/120866373.

[53] H. Wang, C. S. Peskin, and T. C. Elston, *A robust numerical algorithm for studying biomolecular transport processes*, J. Theoret. Biol., 221 (2003), pp. 491–511.

[54] Y. Wang, C. Liu, P. Liu, and B. Eisenberg, *Field theory of reaction-diffusion: Mass action with an energetic variational approach*, Phys. Rev. E, 102 (2020), 062147.

[55] Y. Wang, T.-F. Zhang, and C. Liu, *A two species micro–macro model of wormlike micellar solutions and its maximum entropy closure approximations: An energetic variational approach*, J. Non-Newtonian Fluid Mech., 293 (2021), 104559.

[56] J. WEI, *Axiomatic treatment of chemical reaction systems*, J. Chem. Phys., 36 (1962), pp. 1578–1584.

[57] M. YUAN, W. CHEN, C. WANG, S. WISE, AND Z. ZHANG, *An energy stable finite element scheme for the three-component Cahn-Hilliard-type model for macromolecular microsphere composite hydrogels*, J. Sci. Comput., 87 (2021), 78.

[58] C. ZHANG, J. HUANG, C. WANG, AND X. YUE, *On the operator splitting and integral equation preconditioned deferred correction methods for the "good" Boussinesq equation*, J. Sci. Comput., 75 (2018), pp. 687–712.

[59] C. ZHANG, H. WANG, J. HUANG, C. WANG, AND X. YUE, *A second order operator splitting numerical scheme for the "good" Boussinesq equation*, Appl. Numer. Math., 119 (2017), pp. 179–193.

[60] J. ZHANG, C. WANG, S. M. WISE, AND Z. ZHANG, *Structure-preserving, energy stable numerical schemes for a liquid thin film coarsening model*, SIAM J. Sci. Comput., 43 (2021), pp. A1248–A1272, https://doi.org/10.1137/20M1375656.

[61] S. ZHAO, *Operator splitting ADI schemes for pseudo-time coupled nonlinear solvation simulations*, J. Comput. Phys., 257 (2014), pp. 1000–1021.

[62] S. ZHAO, J. OVADIA, X. LIU, Y.-T. ZHANG, AND Q. NIE, *Operator splitting implicit integration factor methods for stiff reaction–diffusion–advection systems*, J. Comput. Phys., 230 (2011), pp. 5996–6009.